Molecular Nanotechnology & Nanomedicine

http://elynsgroup.com

Research Article Journal of Molecular Nanotechnology and Nanomedicine Open Access

Osseous Regeneration of Periapical Lesions using Rice Straw Nanofibers-Nano Amorphous Calcium Phosphate Composite Hydrogel (*In-Vivo* Study)

Engie M. Safwat[1], Nehal F. Sharaf[1], Abdel Razik H. Farrag[2], Mohamed L. Hassan[3]*, Dalia Y. Zaki[1]

[1]Restorative and Dental Materials Department, National Research Centre, Egypt

[2]Pathology Department, National Research Centre, Egypt

[3]Cellulose and Paper Department, National Research Centre, Egypt

Received Date: January 31, 2020, **Accepted Date:** February 27, 2020, **Published Date:** March 06, 2020.

***Corresponding author:** *Mohamed L. Hassan, Cellulose and Paper Department, National Research Centre, Egypt; E-mail: ml.hassan@nrc.sci.eg*

Abstract

The objective of this study was to investigate the ability of rice straw extracted cellulose nanofibers (CNF) / nano amorphous calcium phosphate (nACP) composite hydrogel, to induce bone regenerationin the periapical lesions of endodontically treated teeth. The in-vivo study was performed through drilling surgical cavities, periapical to endodontically treated molars of experimental dog. Three materials were tested during this study including; CNF hydrogel, nACP powder, and CNF-nACP nanocomposite in 2:1 weight ratio. Periapical bone density analysis was done using Dual-energy X-ray absorptiometry (DXA), in addition, histopathological investigations of the filled periapical bone defect were obtained using H&E and Masson's trichrome (MT) staining. Areas of newly formed collagenous bone, MT stained in green-blue, were measured in multiple fields for each group. The analysis showed that nACP and CNF-nACP nanocomposite hydrogel could form the normal bone density, meanwhile, only CNF-nACP composite presented matured bone and collagen formation ($P < 0.05$). The DXA and histological results indicated that CNF-nACP nanocomposite could have promising osteoconductive potential.

Keywords: Cellulose nanofibers; Nano amorphous calcium phosphate; Osseous regeneration

Introduction

Infection of dental pulp tissue may be a consequence of untreated caries or trauma, causing tissue necrosis [1]. Bacterial infection with its released by-product causes a series of inflammatory and immunological reactions in the periapical area. According to the host's immune response together with the virulence of microbial infection, various grades of periapical lesions could develop. However, no self-healing could occur, where periapical abscess, radicular cysts or periapical granuloma could develop in improperly treated teeth. For the treatment of these cases, elimination or decreasing microbial infection is to be done through efficient chemo-mechanical preparation of the teeth root canals.

On the other hand, large periapical lesions may require surgical approach especially when the lesion is covered by an intact epithelium, separating it from the apical foramen and preventing the drainage of pus through the canal. Recent studies revealed that following regenerative techniques (RT) using bone graft; produce a superior outcome when compared with that without using RT [2]. Bone graft substitutes are used to accelerate periapical healing, to allow healing in compromised clinical situations, and to serve as scaffold for new bone formation [3].

Synthetic biomaterials have been developed as bone graft substitutes, including ceramics e.g., hydroxyapatite and various calcium phosphate compositions [4]. The use of polymeric materials also allowed; better handling, favorable vascularization and provide the capability to carry inorganic bioactive particles into their matrix forming composites [5]. Examples of tested polymers for bone regeneration applications are poly (lactic-co-glycolic acid) [6], gelatin [7], chitosan [8], and collagen [9].

In bone tissue regeneration applications natural polymers proved to have several advantages when compared with synthetic polymers. Natural polymers provide higher biocompatibility, sufficient hydrophilicity, and biodegradability. Cellulose, starch, chitosan, chitin, collagen, gelatin are examples of natural polymers that have been investigated and used for the development of 3D scaffold [10]. The unique properties of cellulose regarding its biocompatibility, non-toxicity, stability to moderate temperature and pH variations and adequate surface chemistry profile were the driving force for its biological applications [11].

Many literatures have focused on injectable gels for bone tissue engineering applications, prepared from different materials such as calcium phosphates combined with methylcellulose [12,13], carboxymethyl cellulose [14,15], hydroxyl propylmethyl cellulose [16,17], silanized-hydroxypropyl methylcellulose [18,19] and bisphosphonated-nanocellulose [20]. Nanocellulose has been also used for bone tissue engineering but the in-vivo studies on experimental animals to test bone tissue regeneration; were rarely done [21,22].

Previous in-vitro study was done to investigate the use of cellulose nanofibers (CNF), isolated from rice straw for the preparation of an injectable hydrogel for bone regeneration [23]. In that study, Tetramethyl pyridine oxyl (TEMPO) oxidized CNF, were mineralized through the incorporation of 50 wt% biphasic calcium phosphate. Cytotoxicity and alkaline phosphatase level tests on osteoblast like-cells were investigated. Results proved that the isolated CNF is a nanocomposite of cellulose nanofibers and silica nanoparticles. The tested materials showed a nontoxic effect on osteoblast-like cells. However, CNF-biphasic calcium phosphate composite hydrogel showed higher cytotoxicity and lower bioactivity when compared to that of neat CNF. For that reason, nACP was used in this study due to its promising bioactivity as revealed in many kinds of literature [24-29].

Therefore, the aim of the present study was to assess the in-vivo biocompatibility and the osteogenic potential of the experimental CNF hydrogel prepared according to Safwat, et al., 2018 [23], loaded by nACP for treatment of periapical lesions of endodontically treated teeth.

Materials and Methods

Rice straw agricultural wastes were collected from local farms in Giza, Egypt and used for the preparation of CNF hydrogel according to Safwat et al, 2018 [23].

The prepared rice straw CNF had dimensions in the range of 4 nm to 8 nm in width and reached up to several microns in length [23]. The isolated CNF was found to be loaded with nano-sized silica (~ 50 nm in diameter) which is naturally intimately embedded in rice straw [30]. Nano Amorphous calcium phosphate (nACP) was purchased from Sigma Aldrich Chemical Company St. Louis, USA. CNF and nACP were mixed such that each 2cm 3 volume of CNF hydrogel (2% dry weight) was added to 1cm 3 in volume (0.2304 gm weight) of nACP.

Grouping of the Tested Materials

Three group samples were tested in this study as follows: group 1: CNF hydrogel, group 2: nACP powder and group 3: CNF-nACPnanocomposite hydrogel.

Sterilization of the Tested materials

Samples were sterilized by gamma-ray irradiation at 25 kGy, using cobalt-60 as irradiation source, with an irradiation dose rate of 1 kGy per hour.

Surgical Procedure

The surgical procedures were conducted according to the protocol approved by the Ethical Committee of the National Research Centre, Cairo, Egypt with the registration number of (18079), and was done in accordance with ISO 10993-6:2016 [31]. The study was done on adult mongrel dogs, weighed 25 ± 1 kg body weight, and aged 1 ± 0.5 years. Dogs were examined thoroughly before the selection and were kept under observation for 2 weeks.

Surgical procedures were carried out under general intramuscular anesthesia injection of ketamine (6.5-13 mg/kg IM, midazolam). Routine infiltration anesthesia of Lindocaina 2% was administered at the surgical sites.

In this study, three molars in the mandibular right side of the dog were endodontically treated. After rubber dam application, the teeth surfaces were disinfected with 2% chlorohexidine gluconate. Root canals were instrumented to the full working length up to size 40 using k-files (Maillefer instruments, Switzerland). 2.6% Sodium hypochlorite (NaOCl) was used as a root canal irrigating solution. The prepared canals were then dried and obturated using guttapercha cones and Ad Seal™ resin sealer (Metabiomed OK, Chungbuk, Korea). A full thickness flap was then elevated in the alveolar ridge to expose the periapical areas of the root canal treated teeth. Seven surgical cavities were drilled periapical to the roots of the endodontically treated teeth using 3-mm diameter surgical drills (Neobiotech Co., Seoul, Korea) with a 30: 1 reduction handpiece at a speed of 1000 RPM. The final torque value was 35 Ncm. For standardization and ethical considerations, all the tested materials were presented in the same dog.

The first two cavities received group 1 samples, the second two cavities received group 2 samples, and the third two cavities received group 3 samples. A fourth cavity was left empty as a control. The flap was repositioned and sutured over the bony cavities (Figure 1). The dogs were fed with a soft diet for the first week postoperatively followed by a regular diet. Sacrifice was done after 15 weeks using high doses of anesthesia and then mandible was dissected for DXA scanning followed by histological examination.

Bone mineral density (BMD)

DXA Norland densitometer (XR-46, USA) Rev. 4.6.4/2.3.1 was used to evaluate bone regeneration and remodeling in each particular periapical region containing one of the three experimental groups. The DXA scanner was adapted for the analysis, such that the entered parameters were set up to measure the human child age of near weight [32]. Measures of bone mineral density (BMD) expressed in g/cm2 were performed for each particular periapical region containing one of the three experimental groups in the separated mandibular right side. All analyses were conducted using high-precision mode DXA at 1-mm scan pitch. Results were expressed as mean BMD of periapical areas in the same group and were compared to the normal bone in the periapical region of the same size.

Figure 1: Experimental samples insertion in the surgical cavities periapical to the endodontically treated roots.

Histological assay

Histological sample preparation: Mandible was fixed in 10% formaldehyde for 24h, rinsed in running tap water for 24h to remove formaldehyde, then incubated with EDTA (pH 7.4) as a decalcifying solution. The decalcification process was performed under continuous shaking and the decalcifying solution was changed weakly. The decalcification procedure was ended when a needle without any force easily penetrated through the bone. Subsequently, samples were washed in running tap water for 24h, followed by dehydration in a series of ethanol and then embedded in paraffin. 5 μm sections were cut using a Leica microtome (Leica, Germany) and placed on glass slides [33].

Staining methods: Hematoxylin and Eosin staining were performed according to GuoY, et al. [34]. Briefly, after deparaffinization and rehydration, the 5 μm longitudinal sections were stained with hematoxylin solution for 5 min followed by 5 dips in 1% acid ethanol (1% HCl in 70% ethanol) and then rinsed in distilled water. The sections were then stained with eosin solution for 3 minutes and followed by dehydration with graded alcohol and clearing in xylene. The mounted slides were then examined and photographed using an Olympus BX51 light microscope (Tokyo, Japan).

Masson's trichrome (MT) staining was also used to identify bone tissue formation and maturation stage [35,36]. Sections were stained in Biebrich scarlet-acid fuchsine solution for 15 minutes and rinsed in distilled water. Sections were then incubated in phosphomolybdic–phosphotungstic acid solution for 15 minutes, transferred directly to aniline blue solution and then stained for 5–10 minutes. Sections were rinsed in distilled water, washed in 1% acetic acid solution for 2–5 minutes, and then rinsed in distilled water. Stained sections were dehydrated; coverslipped with DPX as a mounting medium, to be examined using an Olympus BX51 light microscope. MT dye stains the new collagenous bone in green-blue and the mature osteoid in red; six fields in each group were photographed using a digital camera, analyzed to indicate the area percentage of newly mineralized bone formation.

Statistical analysis

The statistical analyses were carried out using SPSS version

13.0. The significance between means was calculated by the single factor ANOVA. The difference was regarded as significant if the 'P' value was < 0.05.

Results and Discussion

CNF with a diameter close to that of elementary cellulose fibers (~4nm) could be isolated from TEMPO-oxidized cellulose pulp prepared from rice straw. The isolated CNF form injectable gel at 2 wt. % in water [23]. The addition of nACP to CNF gel at the studied concentration of the former did not affect the ease of injectability.

DXA has been demonstrated to measure skeletal maturity [37] and was used to evaluate the effects of pharmaceutical therapy on bone density [38]. BMD of all groups was presented in table 1. A significant decrease in BMD of bone received group 1 was found, as compared with non-cavitated normal bone ($P < 0.05$). However, statistically insignificant differences were found in the results of group 2, group 3 and the non-cavitated normal bone ($P < 0.05$). Results indicate that; both nACP and CNF-nACP composite stimulated the formation of new calcified bone.

Table 1: Mean BMD of the tested periapical areas in all groups. Data presented as mean ± standard error. * Significant decrease at $P < 0.05$ as compared with non-cavitated normal bone. ^{NS} non-significant decrease at $P < 0.05$ as compared with non-cavitated normal bone.

Group Parameter	BMD (g/cm^2)
Non cavitated normal bone	0.7268 ± 0.0145
Bone received group 1	0.6613 ± 0.0097*
Bone received group 2	0.7122 ± 0.0128 ^{NS}
Bone received group 3	0.7027 ± 0.0236 ^{NS}

These primary results were confirmed by the histological examination of H&E and Masson's trichrome dyes. As for the H&E stained sections, the control group revealed the formation of collagen-rich connective tissue. Tissue formation was detected mainly in the intramedular space, with no new bone formation (Figure 2A). Regarding cavities of group 1, almost no regenerated bone in the defect areas were detected, only bundles of collagenous are found (Figure 2B).On the other hand, new regenerated bone volumes filling the defect were detected in cavities of group 2. In this group, osteoblasts were found around the newly formed bone, while few numbers of osteocytes were found inside the newly formed bone indicating its immaturity, hollow areas were detected in the defect area in some samples demonstrating incomplete bone formation (Figure 2C). On the other hand, group 3 showed almost total bone repairing in the defected area. Osteoblasts were found around the newly formed bone, while high numbers of osteocytes were found inside the new bone. New blood vessels were found around the new bone area, indicating full maturity of the formed bone (Figure 2D).

A representative sample of histological sections of different

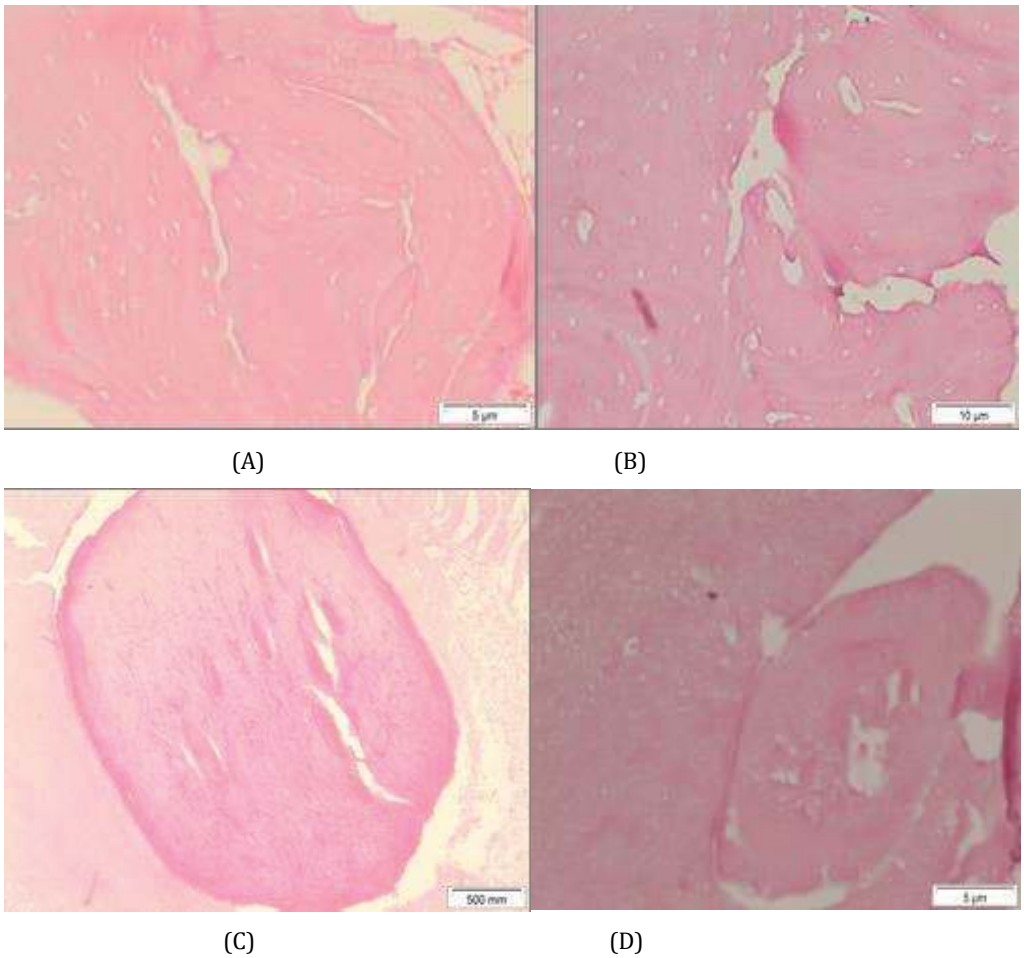

Figure 2: A section in dog's mandibular bone in the periapical region, showing: (A) section of the control group, (B) section of group 1, (C) section of group 2, (D) section of group 3 (H and E, Scale bar 5 µm).

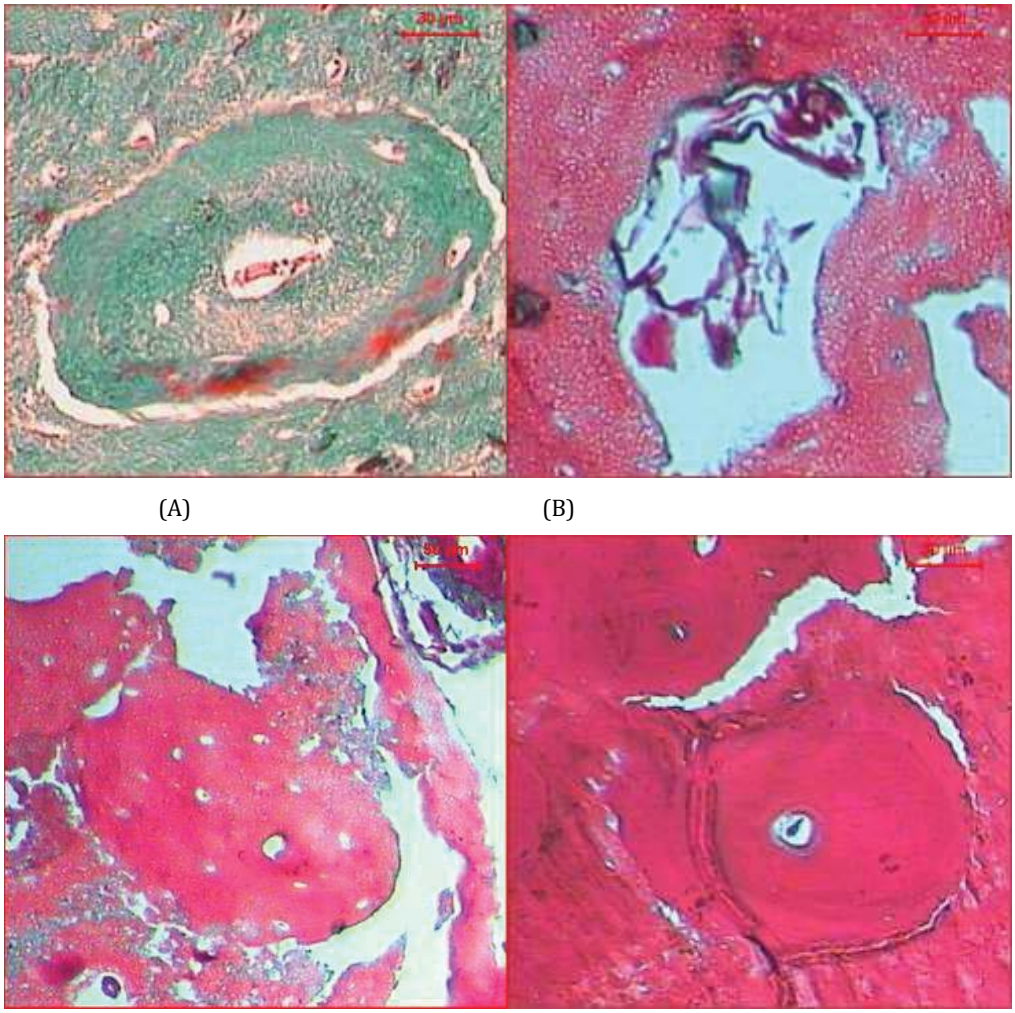

Figure 3: Histological section in the periapical region of dog's mandibular bone showing; (A) section of the control group, (B) section of group 1, (C) section of group 2, (D) section of group 3 (Masson's trichrome staining, Scale bar 30 μm).

groups stained using Masson's trichrome staining was shown in figure 2. Sections of the control group showed no evidence of new bone formation (Figure 3A). Regarding cavities of group 1, only bundles of collagenous were found as revealed by the green-blue color but diminutive regenerated bone (red) was formed (Figure 3B). Cavities of group 2 showed newly regenerated bone filling the defect but of few osteocytes indicating immature bone formation (Figure 3C). On the other hand, cavities of group 3 (Figure 3D) showed both reddish-colored regenerated bone and green-blue collagenous bone formation, with osteocytes inside the newly formed bone indicating bone maturity.

Quantitative measurement of the areas of newly formed collagenous bone, stained in the green-blue stains showed a significant increase at $P < 0.05$ in all groups as compared with the control group, though, a significant decrease of bone formed areas compared with group 1 (Table 2). Although group 1 had the highest collagenous bone formed, yet no regenerated bone has formed, indicating its low osteogenic potential. On the other hand, the lowest green-blue areas revealed by group 2 is due to the regenerated bone formation (red) though not fully matured as indicated by scarce osteocytes. Meanwhile, group 3 had both collagenous and regenerated bone with osteocytes and osteoblasts, indicating favorable conditions for high quality mature bone formation.

Table 2: Areas of newly formed bone of different groups. All data are presented as mean ± SE. *Significant increase at *P< 0.05* as compared with control group. •Significant decrease at *P< 0.05* as compared with group 1.

Parameter Groups	Area^2
Control	497.81 ± 174.65
Group 1	21585.09 ± 1925.67*•
Group 2	719.45 ± 238.73*•
Group 3	1124.77 ± 460.55*•

Such findings indicate the biocompatibility, the osteoconductive potential and the bioactivity of both nACP and CNF-nACP composite hydrogel with the preeminence of CNF-nACP composite. This is probably due to the known role of nACP as a bioapatite forming precursor. Dissolution and precipitation take place at the particle surface in body fluid. Under physiological conditions dissolution process is affected by particle composition, the body fluid mineral supersaturation level, and the implantation site. The nanoscale of the nACP particles and their amorphous structure enhance the dissolution process through their higher total surface area exposed to the surrounding fluids together with the increased reactivity due to their amorphous structure improving their in-vivo osteoconductivity [39].

The presence of well-formed bone filling the defect cavity after using CNF-nACP hydrogel composite may indicate the more favorable effect of using CNF hydrogel together with nACP on bone formation. Such finding is in agreement with results obtained by the study done by Safwat E, et al [23], where nanocellulose hydrogel prepared from rice straw proved to have the ability to induce ossification as indicated by the positive alkaline phosphate assay. The presence CNF with its bioactive role and the known ability of the hydrogel to confine and maintain a high concentration of the loaded active ingredient at the implantation site over an extended period of time; may play a role in increasing the level of bone formation [40].

Conclusion

Within the limitations of the present study, it could be concluded that CNF-nACP nanocomposite hydrogel is a biocompatible material with osteoconductive potential and bioactivity. CNF-nACP nanocomposite hydrogel proved to have a more favorable bone forming effect when compared to nACP powder.

Acknowledgments

The authors would like to acknowledge the financial support of "National Research Centre, Egypt", grant number; AR111402.

Conflict of Interest

Authors declared that they have no conflict of interest.

References

1. Gupta SS, Shetty DC, Urs AB, Nainani P. Role of inflammation in developmental odontogenicpathosis. J Oral Maxillofac Pathol. 2016;20:164.
2. Taschieri S, Del Fabbro M, Testori T, Saita M, Weinstein R. Efficacy of guided tissue regeneration in the management of through-and-through lesions following surgical endodontics: A preliminary study. Int J Periodontics Restorative Dent. 2008;28:265-71.
3. Yoshikawa G, Murashima Y, Wadachi R, Sawada N, Suda H. Guided bone regeneration (gbr) using membranes and calcium sulphate after apicectomy: A comparative histomorphometrical study. Int Endod J. 2002;35:255-263.
4. Daugela P, Pranskunas M, Juodzbalys G, Liesiene J, Baniukaitiene O, Afonso A, et al. Novel cellulose/hydroxyapatite scaffolds for bone tissue regeneration: In vitro and in vivo study. Tissue Eng Regen Med. 2018;12:1195-1208.
5. Fragal EH, Cellet TS, Fragal VH, Witt MA, Companhoni MV, Ueda-Nakamura T, et al. Biomimetic nanocomposite based on hydroxyapatite mineralization over chemically modified cellulose nanowhiskers: An active platform for osteoblast proliferation. Int J Biol Macromol. 2019;125:133-142.
6. Kim TG, Park TG. Biomimicking extracellular matrix: Cell adhesive rgd peptide modified electrospun poly (d, l-lactic-co-glycolic acid) nanofiber mesh. Tissue Eng. 2006;12:221-233.
7. Ishida K, Kuroda R, Miwa M, Tabata Y, Hokugo A, Kawamoto T, et al. The regenerative effects of platelet-rich plasma on meniscal cells in vitro and its in vivo application with biodegradable gelatin hydrogel. Tissue Eng. 2007;13:1103-1112.
8. Kim I-Y, Seo S-J, Moon H-S, Yoo M-K, Park I-Y, Kim B-C, Cho C-S. Chitosan and its derivatives for tissue engineering applications. Biotechnol. 2008;26:1-21.
9. Ferreira AM, Gentile P, Chiono V, Ciardelli G. Collagen for bone tissue regeneration. Acta Biomater. 2012;8:3191-3200.
10. Wang S, Lu A, Zhang L. Recent advances in regenerated cellulose materials. ProgPolym Sci. 2016;53:169-206.
11. Lin N, Dufresne A. Nanocellulose in biomedicine: Current status and future prospect. Eur Polym J. 2014;59:302-325.
12. Kim MH, Kim BS, Park H, Lee J, Park WH. Injectable methylcellulose hydrogel containing calcium phosphate nanoparticles for bone regeneration. Int J Biol Macromol. 2018;109:57-64.
13. Park H, Kim MH, Yoon YI, Park WH. One-pot synthesis of injectable methylcellulose hydrogel containing calcium phosphate nanoparticles. Carbohydr. 2017;157:775-783.
14. Song S-H, Yun Y-P, Kim H-J, Park K, Kim SE, Song H-R. Bone formation in a rat tibial defect model using carboxymethyl cellulose/bioc/bone morphogenic protein-2 hybrid materials. Biomed Res Int. 2014;2014:230152.
15. De Freitas DG, Osthues RM, da Silva SN. Study of the cytotoxicity of a composite of carboxymethylcellulose (CMC) and a BioCeramic (biphasic calcium phosphate-BCP) injection for use in articular cartilage repair, in: Key Engineering Materials, vol. 493, Trans Tech Publ, 2012, pp. 703-708.
16. Struillou X, Boutigny H, Badran Z, Fellah BH, Gauthier O, Sourice S, et al. Treatment of periodontal defects in dogs using an injectable composite hydrogel/biphasic calcium phosphate. J Mater Sci: Mater Med. 2011;22:1707-1717.
17. Daculsi G, Uzel A, Weiss P, Goyenvalle E, Aguado E. Developments in injectable multiphasic biomaterials. The performance of microporous biphasic calcium phosphate granules and hydrogels. J Mater Sci Mater Med. 2010;21:855-861.
18. Fellah BH, Weiss P, Gauthier O, Rouillon T, Pilet P, Daculsi G, et al. Bone repair using a new injectable self-crosslinkable bone substitute. J Orthop Res. 2006;24:628-635.
19. Trojani C, Boukhechba F, Scimeca J-C, Vandenbos F, Michiels J-F, Daculsi G, et al. Ectopic bone formation using an injectable biphasic calcium phosphate/si-hpmc hydrogel composite loaded with undifferentiated bone marrow stromal cells. Biomaterials. 2006;27:3256-3264.
20. Nishiguchi A, Taguchi T. An osteoclast-responsive, injectable bone of bisphosphonated-nanocellulose that regulates osteoclast/osteoblast activity for bone regeneration. Biomacromolecules. 2019;20:1385-1393.
21. Kumbhar JV, Jadhav SH, Bodas DS, Barhanpurkar-Naik A, Wani MR, Paknikar KM, et al. In vitro and in vivo studies of a novel bacterial cellulose-based acellular bilayer nanocomposite scaffold for the repair of osteochondral defects. Int J Nanomedicine. 2017;12:6437-6459. doi: 10.2147/IJN.S137361.
22. Saska S, Barud H, Gaspar A, Marchetto R, Ribeiro SJL, Messaddeq Y. Bacterial cellulose-hydroxyapatite nanocomposites for bone regeneration. Int Jbiomater. 2011; 2011:175362. doi: 10.1155/2011/175362.
23. Safwat E, Hassan ML, Saniour S, Zaki DY, Eldeftar M, Saba D, et al. Injectable tempo-oxidized nanofibrillated cellulose/biphasic calcium phosphate hydrogel for bone regeneration. J Biomater Appl. 2018;32:1371-1381.
24. Mahamid J, Aichmayer B, Shimoni E, Ziblat R, Li C, Siegel S, et al. Mapping amorphous calcium phosphate transformation into crystalline mineral from the cell to the bone in zebrafish fin rays. Proc Natl Acad Sci U S A. 2010;107:6316-21. doi: 10.1073/pnas.0914218107.
25. Nudelman F, Pieterse K, George A, Bomans PH, Friedrich H, Brylka LJ, et al. The role of collagen in bone apatite formation in the presence of hydroxyapatite nucleation inhibitors. Nat Mater. 2010;9(12):1004-9. doi: 10.1038/nmat2875.
26. Mahamid J, Sharir A, Gur D, Zelzer E, Addadi L, Weiner S. Bone mineralization proceeds through intracellular calcium phosphate loaded vesicles: A cryo-electron microscopy study. J Struct Biol. 2011;174:527-535.
27. Boonrungsiman S, Gentleman E, Carzaniga R, Evans ND, McComb DW, Porter AE, et al. The role of intracellular calcium phosphate in osteoblast-mediated bone apatite formation. Proc Natl Acad Sci U S A. 2012; 109(35):14170-5. doi: 10.1073/pnas.1208916109.
28. Nitiputri K, Ramasse QM, Autefage H, McGilvery CM, Boonrungsiman

S, Evans ND, et al. Nanoanalytical electron microscopy reveals a sequential mineralization process involving carbonate-containing amorphous precursors. ACS nano. 2016;10(7):6826-6835. doi: 10.1021/acsnano.6b02443.

29. Kerschnitzki M, Akiva A, Shoham AB, Asscher Y, Wagermaier W, Fratzl P, et al. Bone mineralization pathways during the rapid growth of embryonic chicken long bones. J Struct Biol. 2016;195(1):82-92. doi: 10.1016/j.jsb.2016.04.011.

30. Hassan ML, Mathew AP, Hassan EA, El-Wakil NA, Oksman K. Nanofibers from bagasse and rice straw: Process optimization and properties. Wood Sci Technol. 2012;46:193-205.

31. Standardization of ISO 10993–6: 2016: Biological evaluation of medical devices—part 6: Tests for local effects after implantation. 2016.

32. Grier S, Turner A, Alvis M. The use of dual-energy x-ray absorptiometry in animals. Investig Radiol. 1996;31:50-62.

33. González-Chávez SA, Pacheco-Tena C, Macías-Vázquez CE, Luévano-Flores E. Assessment of different decalcifying protocols on osteopontin and osteocalcinimmunostaining in whole bone specimens of arthritis rat model by confocal immunofluorescence. Int J Clin Exp Pathol. 2013;6(10):1972.

34. Guo Y, Wang L, Ma R, Mu Q, Yu N, Zhang Y, et al. Jiangtang xiaoke granule attenuates cathepsin k expression and improves igf-1 expression in the bone of high fat diet induced kk-ay diabetic mice. Life sci. 2016;148:24-30. doi: 10.1016/j.lfs.2016.02.056.

35. Xiong Z, Ding H, Li C, Tian Y, Xu Z. Effect of decalcification on immunohistochemical staining of osseous and soft tissue. Chinese Journal of Diagnostic Pathology. 2000;7:45-47.

36. Hatakeyama J, Anan H, Hatakeyama Y, Matsumoto N, Takayama F, Wu Z, et al. Induction of bone repair in rat calvarial defects using a combination of hydroxyapatite with phosphatidylserine liposomes. J Oral Sci. 2019;61:111-118.

37. Płudowski P, Lebiedowski M, Lorenc RS. Evaluation of the possibility to assess bone age on the basis of dxa derived hand scans—preliminary results. Osteoporosis int. 2004;15(4):317-322.

38. Barnes C, Newall F, Ignjatovic V, Wong P, Cameron F, Jones G, et al. Reduced bone density in children on long-term warfarin. Pediatrics. 2005;57(4):578.

39. Mostafa AA, Zaazou MH, Chow LC, Mahmoud AA, Zaki DY, Basha M, et al. Injectable nanoamorphous calcium phosphate based in situ gel systems for the treatment of periapical lesions. Biomed Mater. 2015;10(6):065006. doi: 10.1088/1748-6041/10/6/065006.

40. Hoare TR, Kohane DS. Hydrogels in drug delivery: Progress and challenges. Polymer. 2008;49(8):1993-2007.

***Corresponding author:** Mohamed L. Hassan, Cellulose and Paper Department, National Research Centre, Egypt; E-mail: ml.hassan@nrc.sci.eg.

Received Date: January 31, 2020, **Accepted Date:** February 27, 2020, **Published Date:** March 06, 2020.

Citation: Safwat EM, Sharaf NF, Farrag ARH, Hassan ML, Zaki DY (2020) Osseous Regeneration of Periapical Lesions using Rice Straw Nanofibers-Nano Amorphous Calcium Phosphate Composite Hydrogel (*In-Vivo* Study). J Mol Nanot Nanom 2(1): 109.